Available online at www.sciencedirect.com
SCIENCE DIRECT®
Composite Structures 68 (2005) 109–117
COMPOSITE STRUCTURES
www.elsevier.com/locate/compstruct

NARMAX model representation and its application to damage detection for multi-layer composites

Z. Wei, L.H. Yam *, L. Cheng

Department of Mechanical Engineering, The Hong Kong Polytechnic University, Hung Hom, Kowloon, Hong Kong

Available online 9 April 2004

Abstract

The estimation of nonlinear autoregressive moving average with exogenous input (NARMAX) models for vibrating multi-layer composite plates is presented and used to assess internal delamination in the plates. Both static and dynamic tests are carried out to investigate the nature of the nonlinearity of the composite system. The nonlinear nature and order of nonlinearity are then approximated, and used to restrict the search space of the potential NARMAX model. After the structure and terms of the NARMAX model are identified, all coefficients are calculated for the intact plate. Delamination in the plate is assessed according to the coefficient variations in the model using the measured input/output data for the damaged system. Results show that the model output prediction is in agreement with the test data. The proposed method is available to discover and assess severity and location of delamination in the composite plates.

Keywords: Multi-layer composite; Nonlinearity; NARMAX model; Damage detection

1. Introduction

With the wide application of composites in aerospace and vehicle industries, civil engineering and other mechanical components, the nondestructive testing (NDT) or online damage detection for composite structures is absolutely necessary for service safety. Fiber-reinforced laminae are the most frequently used composites. Due to imperfections introduced during the manufacturing process or induced by external repeated or impact loads, delamination is a major concern for in-service composites and has the most critical potential danger in the hidden state, i.e., internal delamination. Early detection of initial damage can prevent a catastrophic failure or structural deterioration beyond repair. It is, therefore, critical to detect the damage for practical composites or structures, especially at the early stage [1–5].

A number of studies have been carried out to show the effectiveness of dynamic response measurements for NDT of composites. Vibration-based NDT method has been developed in order to detect the damage by dynamic analysis [6]. The basic idea in vibration-based damage detection is that the modal parameters depend on the physical properties of the structure to be inspected. Therefore, changes in physical properties of a structure due to damage can result in detectable variations in its modal parameters, such as natural frequencies, mode shapes and modal damping. However, as the damage-induced variation of modal parameters is always slight, it is not always practical to detect damage, especially in the early or initial state using this method.

Because of its ability to learn from past experiences and to memorize patterns in the form of an associative memory, neural networks (NNs) have been applied successfully in many fields. The candidate models for structures with various types of damage are designated as patterns for damage identification. These different patterns are organized into pattern classes according to the location and severity of damage. To identify the status of a structure, so as to detect damage or to monitor the health of the structure the NNs must be trained using a great number of input–output data of intact and various damaged samples. Due to the limitation of measured signals of dynamic responses from real-world structure under different episodes of damage, the model-based neural networks (MBNNs) are

* Corresponding author. Tel.: +852-2766-7820; fax: +852-2365-4703.
E-mail address: mmlhyam@polyu.edu.hk (L.H. Yam).

0263-8223/$ - see front matter © 2004 Published by Elsevier Ltd.
doi:10.1016/j.compstruct.2004.03.005

proposed [7–9]. Since the effectiveness of the MBNN system is dependent on the accuracy of the structural model, it is helpful for accurately modeling the practical structure to investigate the model obtained by experimental data.

Due to the complication of material composition, it is difficult to establish accurate analytical models for multi-layer composites. Therefore, the computational model established according to experimental data plays an important role in the implement of damage detection. According to our experimental investigation, the relationship between input and output is nonlinear for multi-layer composite structure. Several authors have studied the realization problem for nonlinear systems and some interesting results have been obtained. Especially for nonlinear discrete system, Leontaritis and Billings have proposed the nonlinear, autoregressive, moving average exogenous (NARMAX) structure as a general parametric form for modeling nonlinear system [10]. NARMAX models describe the nonlinear systems in terms of difference equations relating the current output to combinations of inputs and past outputs. Although it is capable of describing a wide variety of nonlinear systems, it has been used mainly for control problem, where the main objective is to achieve a simple system description.

This paper deals with the NARMAX model of multi-layer composite system in order to carry out damage detection. Based on nonparametric analysis on nonlinear nature test and order approximation of the nonlinearity the NARMAX model is constructed, while the orthogonal estimation algorithm is used to select the model terms according to the error reduction ratio [11]. The computation code is programmed to identify the model structure and estimate parameters. The proposed model is validated using different input/output signals. The applicability of this model for damage detection of some samples is then investigated according to the parameter variations of the model. The results show that the proposed model is well suited to identify the dynamic behavior of multi-layer composite systems and effective to detect internal delamination even at its early state.

2. Nonlinearity analysis on multi-layer composites

2.1. Sample description

Samples of 16-layer carbon fiber-reinforced epoxy plates are prepared. Each sample has an area of 240×180 mm^2 in the orientation of $[0/0/90/90/0/0/90/90]_s$. The laminate is fabricated using TC12K33/S-1 prepreg tapes with a thickness of 0.13 mm. Each damaged sample is delaminated at a specified position by inserting teflon films with a thickness of 0.015 mm as shown in Fig. 1. The teflon film is inserted between the forth and fifth layers when the laminate is fabricated. Simply supported boundary condition is adopted during experiment.

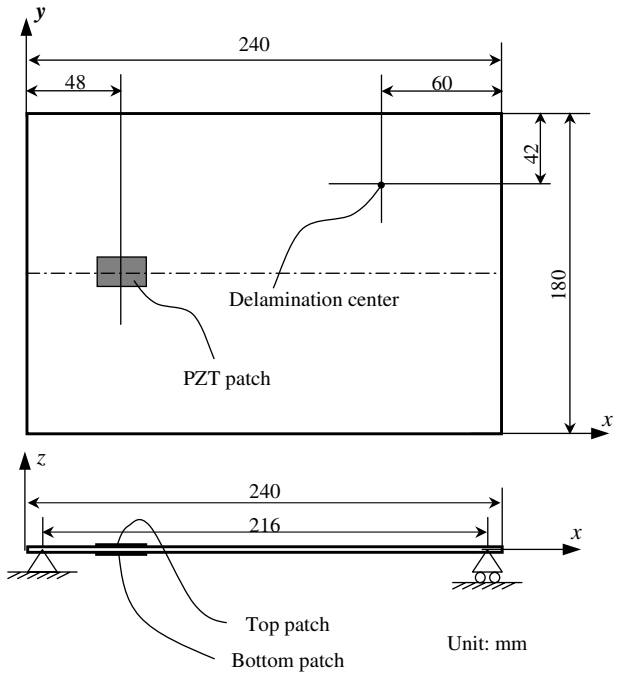

Fig. 1. Geometry and delamination position of the composite system.

2.2. Static analysis

To approximate the nonlinearity of the system, several step inputs of different amplitudes are applied, and then the nonlinear behavior of the system is determined by the relationship between the values of the inputs and outputs. The static load–strain test is used to investigate the behavior of the system. A concentrated compressive load along the opposite of z-direction is applied at the point with coordinates $x = 184$ mm and $y = 168$ mm on the top surface. The strain ε_x along x-direction is measured at the point with coordinates $x = 48$ mm and $y = 90$ mm on the top surface. Fig. 2 shows the strain–load relationship of the intact specimen. It is clear, from the shape of the graph, that the relationship is nonlinear. According to the measured data, using the 4-order polynomial fit the solid line in Fig. 2 can be obtained.

2.3. Dynamic analysis

Periodic signal tests are used to investigate the nonlinear nature of the composite system. According to the spectral properties of the signals it is possible to detect and qualify the dynamic behavior of the nonlinearity in a system by examining the additional frequency contributions generated at the system output by nonlinearity [12]. Dynamic test for the intact sample is conducted

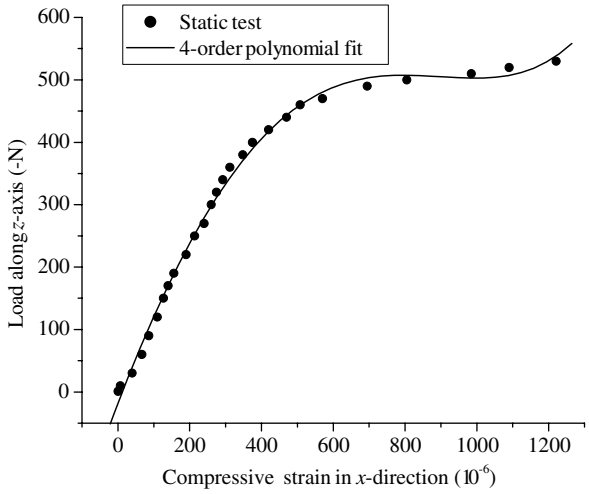

Fig. 2. Strain–load plot obtained by static test with polynomial fit for the intact plate sample.

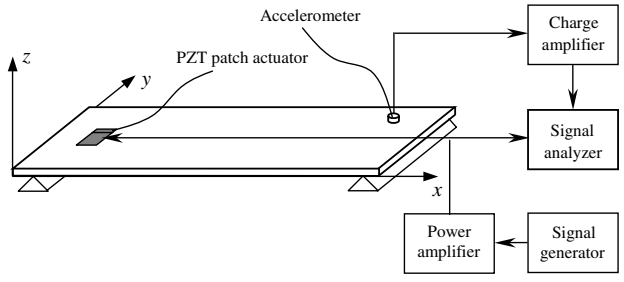

Fig. 3. The experimental set up for dynamic measurement of the composite system.

using the set-up as illustrated by Fig. 3. Two piezoelectric patches with a thickness of 0.28 mm and a size of 15×25 mm^2 are bonded on the top and bottom surfaces, respectively as actuators (the center of the bounded area is just at the point with coordinates $x = 48$ mm and $y = 90$ mm). An accelerometer (Endevco 22) is used as the transducer and adhered to the point with coordinates $x = 184$ mm and $y = 168$ mm. The exciting signal is generated by a waveform generator (TTi TGA1241). A power amplifier (TreK 603) and a charge amplifier (B&K 2635) are used to enhance signals from the generator and transducer, respectively. Both the exciting and response signals are recorded and analyzed by an FFT spectrum analyzer (B&K 3550).

The experimental results also show the nonlinear nature of the system, because the response of the intact system to a harmonic excitation includes not only main harmonic composition, but also the super- and hypo-harmonic compositions of exciting frequency. Fig. 4 shows the relationship between the amplitudes of excitation and response when the exciting signal is sinusoidal with a frequency of 200 Hz. In this figure, the vertical coordinates are the root-mean-square values (RMS) of the acceleration response signals, and the solid

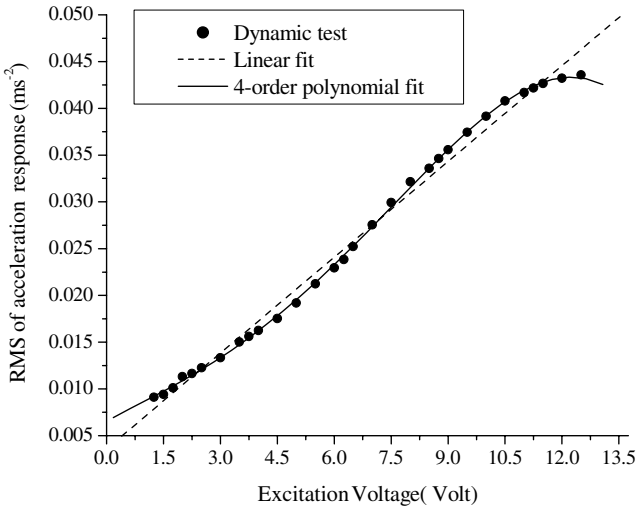

Fig. 4. Excitation-response plot for the intact composite system.

line represents the fourth-order polynomial fit. Therefore, the analysis performed on the available data of both static and dynamic tests indicates the existence of a fourth-order nonlinearity in the mentioned composite system. This information will be used in the next section to identify a parametric nonlinear model capable of representing the dynamic behavior for the multi-layer composite cantilever plates.

3. Estimation algorithm for NARMAX model

Having detected the nonlinearity, the development of a global nonlinear model for the composite system is needed. The NARMAX model for describing the input–output relationship of the nonlinear single-input single-output (SISO) system can be written as

$$y(k) = F^4(y(k-1),\ldots,y(k-n_y),x(k-d),\ldots, x(k-n_x),e(k-1),\ldots,e(k-n_e)) + e(k) \quad (1)$$

where F^4 is a fourth-order polynomial function, x is the exogenous input, y is the output, and e is the noise signal, i.e., the prediction error. n_y, n_x, and n_e are the auto-regressive, exogenous input and moving average orders, respectively. d represents the system time delay.

Just as parameter estimation, the NARMAX model identifies both the structure and the parameters of an unknown nonlinear system. Therefore, after identification of the system nonlinearity, estimating the system parameters is a vital stage.

3.1. Parameter estimation using orthogonal estimator

Detecting which terms are significant and should be included in the model is very important. There exist several structure detection and parameter estimation

algorithms as part of the NARMAX methodology [10]. The orthogonal estimator [13,14] will be used here to estimate structure and parameters of the system, since it is simple to implement and to use. An m-dimensional estimation problem can be reduced to m one-dimensional problems by the orthogonal algorithm, because it allows each coefficient in the model to be estimated independently of the other terms and provides an indication of the contribution that the term makes to the system output.

Suppose there are n_θ process terms in the model of Eq. (1), the NARMAX model can be represented as

$$y(k) = \sum_{i=1}^{n_\theta} \theta_i p_i(k) + e(k) \tag{2}$$

where $p_i(k)$ describes the variable of a term with coefficient θ_i in the model of Eq. (1). Rather than directly estimating θ_i the orthogonal algorithm operates on an equivalent auxiliary model as

$$y(k) = \sum_{i=1}^{n_\theta} g_i w_i(k) + e(k) \tag{3}$$

where $w_i(k)$'s are constructed to be orthogonal over the data record. Because of the orthogonality the parameter vector can be estimated by computing one parameter estimation at a time. The parameters g_i's are estimated by implementing the orthogonal estimator [11]. The algorithm is simple and easy to implement as the auxiliary regressors $w_i(t)$ are orthogonal. Numerical ill-condition can be avoided by deleting $w_j(k)$ if $\sum w_j^2(k)$ for all data points is less than some threshold. The prediction errors must be estimated from Eq. (3) as [13]

$$\hat{e}(k) = y(k) - \sum_{i=1}^{n_\theta} g_i w_i(k) \tag{4}$$

and an estimate of $\sigma^2 = E[e^2(k)]$, i.e., the mathematical prediction of estimation error, can be obtained by

$$\widehat{\sigma} = \sqrt{\frac{1}{N - n_\theta} \sum_{k=1}^{N} e^2(k)} \tag{5}$$

where N represents the number of data points.

3.2. Term selection method

Although the orthogonal algorithm presented above can estimate all the unknown coefficients in the model of Eq. (1), the exclusion of some terms is helpful for simplifying the model. This can be achieved by computing the error reduction ratio for each term by [13]

$$[eRR]_i = \frac{\hat{g}_i^2 \sum_{k=1}^{N} w_i^2(k)}{\sum_{k=1}^{N} y^2(k)} \times 100\% \tag{6}$$

where $\hat{g}_i$ is the estimate of g_i in Eq. (3). As $[eRR]_i$ represents the relative reduction in mean squared error, which would result from including the ith term $g_i w_i(k)$ in Eq. (3) (i.e., $\theta_i p_i(k)$ in the NARMAX model of Eq. (2)), it is tested against a threshold and the ith term is included in the model only if $[eRR]_i$ exceeds the threshold.

If consider all the possible $p_i(k)$ $(i = 1, 2, \ldots, n_\theta)$ as candidates for $w_1(k)$, by finding

$$[eRR]_1^j = \max\{[eRR]_1^i, 1 \leqslant i \leqslant n_\theta\} \tag{7}$$

where

$$[eRR]_1^i = \frac{(\hat{g}_1^i)^2 \sum_{k=1}^{N} (w_1^i(k))^2}{\sum_{k=1}^{N} y(k)^2}; \quad \hat{g}_1^i = \frac{\sum_{k=1}^{N} w_1^i(k) y(k)}{\sum_{k=1}^{N} (w_1^i(k))^2};$$
$$w_1^i(k) = y(k) \tag{8}$$

the first term included in the model is selected as $w_1(k) = w_1^j(k)$, $\hat{g}_1 = \hat{g}_1^j(k)$ and $[eRR]_1 = [eRR]_1^j$ associated with $p_j(k)$. Thus, for $i = 1, \ldots, n_\theta$, $i \neq j$ compute

$$[eRR]_2^i = \frac{(\hat{g}_2^i)^2 \sum_{k=1}^{N} (w_2^i(k))^2}{\sum_{k=1}^{N} y(k)^2}; \quad \hat{g}_2^i = \frac{\sum_{k=1}^{N} w_2^i(k) y(k)}{\sum_{k=1}^{N} (w_2^i(k))^2};$$
$$w_2^i(k) = p_i(k) - \alpha_{12}^i w_1(k) \tag{9}$$

where

$$\alpha_{12}^i = \frac{\sum_{k=1}^{N} w_1(k) p_i(k)}{\sum_{k=1}^{N} w_1^2(k)} \tag{10}$$

$$[eRR]_2^l = \max\{[eRR]_2^i, 1 \leqslant i \leqslant n_\theta, i \neq j\} \tag{11}$$

is obtained, and then, the second term is selected as $w_2(k) = w_2^l(k) = p_l(k) - a_{12}^l w_1(k)$, $\alpha_{12} = \alpha_{12}^l$, $\hat{g}_2 = \hat{g}_2^l(k)$ and $[eRR]_2 = [eRR]_2^l$ associated with $p_l(k)$. Suppose C_d and C_e are the thresholds for the process and noise terms, respectively, the above procedure will be terminated at any step, say q, when $[eRR]_q < C_d$ (or C_e) or when the total parameter set has been searched. Once term selection is completed, the coefficient of each selected term can be calculated by the backward algorithm

$$\theta_{\mathrm{ns}} = g_{\mathrm{ns}}, \quad \theta_i = g_i - \sum_{j=i+1}^{\mathrm{ns}} \alpha_{ij} \theta_j \quad (\mathrm{ns} - 1 \geqslant i \geqslant 1) \tag{12}$$

where ns is the number of all selected terms of the NARMAX model.

Based on the above description, a program code is developed for term selection and coefficient determination of NARMAX model. Fig. 5 shows the approach of the above forward regression algorithm with a noise model estimator.

4. NARMAX model description for multi-layer composites

4.1. Structure identification of NARMAX model

To initially identify the best linear model is helpful for a suitable choice of n_x, n_y and n_e as well as term structure in the NARMAX model of Eq. (1).

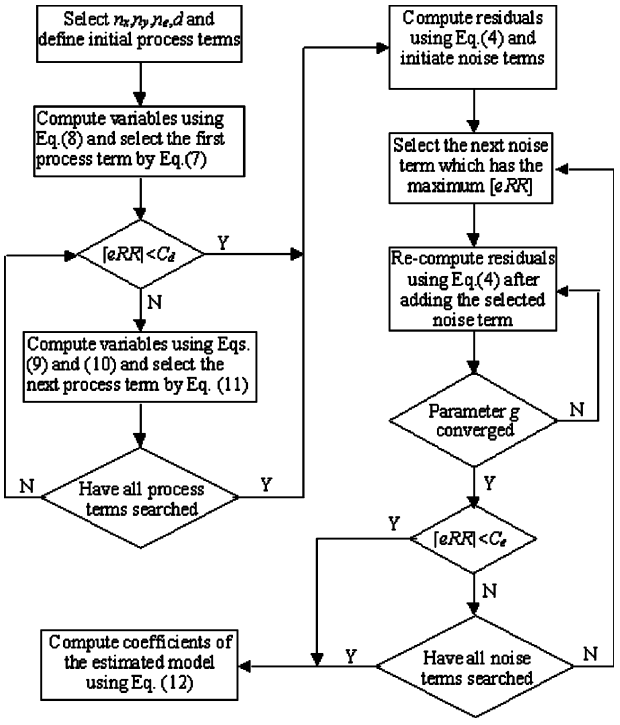

Fig. 5. Flowchart of the orthogonal estimator for NARMAX model.

A white noise signal with a bandwidth of 1–1600 Hz is used as the input for the intact sample described in Section 2. Fig. 6 shows the data records of input and output. For each signal, 2048 points are recorded within 1 s. Table 1 lists the computation results of prediction errors obtained using Eq. (5) for different time delay and forward orders. For simplicity, the same forward orders of input, output and noise terms are adopted. It is seen that when the time delay is 1, as shown by the bold values in Table 1, σ reaches the minimum for almost all forward orders. The table also shows that σ will nearly monotonically decrease with the increase of forward order until it reaches 12 (as shown by the bold values in

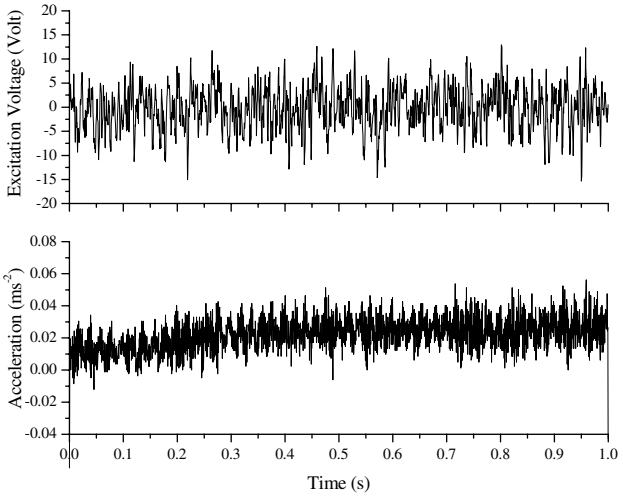

Fig. 6. Input and output of the data records used in modeling for the composite system.

the table), and go up slightly after this order when $d = 1$. Therefore, the time delay of 1 will be used to fit the NARMAX model and an appropriate model order will be $n_x = n_y = n_e = 12$.

Based on the above-mentioned initial guess of n_x, n_y, n_e and d the linear model is estimated by selecting $C_d = 10^{-3}$ and $C_e = 10^{-4}$. The results are summarized in Table 2, where err represents the root-mean-square error calculated using

$$\mathrm{err} = \frac{1}{N}\sqrt{\sum_{k=1}^{N}\hat{e}^2(k)} \tag{13}$$

It is seen that 16 process terms and 9 noise terms have been selected. The root-mean-square errors decrease with the increase of the selected terms, and the decrease rate becomes slow with the completion of the selection.

Following the above suggestions of the model structure and the initial values of forward order and time

Table 1
Values of σ for different ARMAX models for the intact plate

Forward order (n_x)	Time delay (d)							
	0	1	2	3	4	5	6	Average
1	1.02E−2	**9.85E−3**	9.85E−3	9.85E−3	9.85E−3	9.85E−3	9.85E−3	9.90E−3
2	9.99E−3	**9.82E−3**	9.82E−3	9.82E−3	9.82E−3	9.82E−3	9.82E−3	9.84E−3
3	7.45E−3	**7.46E−3**	7.55E−3	7.83E−3	7.91E−3	7.91E−3	7.91E−3	7.72E−3
4	7.14E−3	**7.14E−3**	7.18E−3	7.50E−3	7.50E−3	7.41E−3	7.41E−3	7.33E−3
5	7.22E−3	**7.22E−3**	7.22E−3	7.49E−3	7.49E−3	7.39E−3	7.39E−3	7.35E−3
6	7.03E−3	**7.03E−3**	7.03E−3	6.91E−3	6.91E−3	7.01E−3	7.01E−3	6.99E−3
7	6.83E−3	**6.83E−3**	6.83E−3	6.79E−3	6.95E−3	6.97E−3	6.97E−3	6.88E−3
8	6.05E−3	**6.16E−3**	6.16E−3	6.05E−3	6.18E−3	6.21E−3	6.21E−3	6.15E−3
9	5.51E−3	**5.66E−3**	5.66E−3	6.08E−3	6.23E−3	6.00E−3	6.00E−3	5.88E−3
10	4.65E−3	**4.10E−3**	4.66E−3	4.56E−3	4.80E−3	5.06E−3	5.06E−3	4.70E−3
11	3.96E−3	**3.80E−3**	3.96E−3	4.48E−3	4.48E−3	4.77E−3	4.77E−3	4.32E−3
12	**3.94E−3**	**3.73E−3**	**3.94E−3**	**4.48E−3**	**4.48E−3**	**4.78E−3**	**4.78E−3**	**4.30E−3**
13	4.10E−3	**3.77E−3**	4.12E−3	4.86E−3	4.86E−3	4.88E−3	4.88E−3	4.50E−3

Table 2
Results of ARMAX model estimation for the intact composite system

i	$p_i(k)$	θ_i	err	i	$p_i(k)$	θ_i	err	i	$p_i(k)$	θ_i	err
1	$y(k-3)$	4.92E−1	6.61E−3	9	$x(k-3)$	−1.68E−3	3.67E−3	17	$e(k-7)$	−3.33E−1	2.46E−3
2	$y(k-11)$	4.81E−1	5.60E−3	10	$x(k-1)$	−7.05E−4	3.52E−3	18	$e(k-2)$	3.88E−1	2.44E−3
3	$y(k-10)$	−5.58E−1	5.40E−3	11	$y(k-6)$	2.85E−1	3.43E−3	19	$e(k-11)$	−2.53E−1	2.40E−3
4	$y(k-7)$	4.39E−1	4.58E−3	12	$y(k-9)$	−1.92E−1	3.34E−3	20	$e(k-6)$	−3.24E−1	2.28E−3
5	$x(k-4)$	2.91E−4	4.40E−3	13	$y(k-1)$	1.34E−1	3.21E−3	21	$e(k-10)$	1.42E−1	2.25E−3
6	$x(k-8)$	1.06E−3	4.24E−3	14	$y(k-8)$	−2.19E−1	2.95E−3	22	$e(k-3)$	−1.30E−1	2.25E−3
7	$x(k-2)$	1.96E−3	3.99E−3	15	$y(k-2)$	1.36E−1	2.67E−3	23	$e(k-12)$	−2.29E−1	2.23E−3
8	$x(k-9)$	−4.17E−4	3.78E−3	16	$x(k-7)$	−5.01E−4	2.52E−3	24	$e(k-4)$	2.03E−1	2.20E−3
								25	$e(k-1)$	1.81E−1	**2.14E−3**

delay, the NARMAX model is estimated using the same data and thresholds as those used in linear estimation.

4.2. NARMAX model and its validation

As the fourth-order polynomial model, there are hundreds of possible terms to be selected, but Table 3 indicates that only 34 of them are significant. Table 3 shows that 4 and 5 nonlinear terms have been added to the model for terms of process and noise, respectively. Using the NARMAX model the final root-mean-square errors err is reduced by 10.75% in comparison with the ARMAX model. Fig. 7 shows the model output of acceleration response to random excitation for the intact specimen. It is seen that the NARMAX model has a better prediction of the acceleration data than the ARMAX model.

To investigate the robustness of the proposed model, the acceleration response to sinusoidal sweep signal is also measured for the same composite system as used to estimate the model as illustrated in Table 3. Let the percentage variance accounted for (VAF) by the NARMAX model be defined as

$$\mathrm{VAF} = \left(1 - \frac{\sum_{k=1}^{N} e^2(k)/N}{\sum_{k=1}^{N} y^2(k)/N}\right) \times 100\% \qquad (14)$$

Using the recorded data of sinusoidal excitation as input the model VAF is 98.4%, i.e., the predicted output

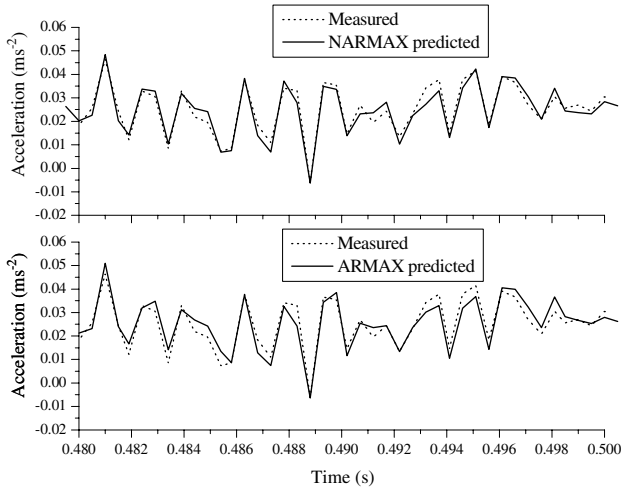

Fig. 7. The predicted outputs of ARMAX and NARMAX models for the intact composite system.

of the proposed NARMAX model matches the measured output with over 98% VAF in this case. Fig. 8 shows the comparison between the outputs of the NARMAX model and the tested data. It is clear that the proposed model can predict the output well when the input is sinusoidal signal although the model is determined using the band-limited white noise signal for the identical composite system. Therefore, the model is

Table 3
Results of NARMAX model estimation for the intact composite system

i	$p_i(k)$	θ_i	err	I	$p_i(k)$	θ_i	err	i	$p_i(k)$	θ_i	err
1	$y(k-3)$	4.58E−1	6.61E−3	12	$x(k-1)$	1.33E−1	3.47E−3	23	$e(k-1)$	5.95E−1	2.39E−3
2	$y(k-11)$	5.22E−1	5.60E−3	13	$y^2(k-8)$	−3.59E+0	3.31E−3	24	$e^3(k-1)$	−1.39E+3	2.33E−3
3	$y^2(k-10)$	−2.69E−0	5.37E−3	14	$y^3(k-9)$	−8.49E+1	3.22E−3	25	$e(k-8)$	−2.25E−1	2.29E−3
4	$y(k-7)$	3.59E−1	4.70E−3	15	$y(k-1)$	1.07E−1	3.11E−3	26	$e^4(k-7)$	2.23E+3	2.26E−3
5	$y(k-10)$	−3.70E−1	4.55E−3	16	$x(k-3)$	−1.35E−3	2.99E−3	27	$e^2(k-11)$	1.20E+1	2.23E−3
6	$x(k-4)$	−3.28E−5	4.39E−3	17	$x(k-1)$	−5.74E−4	2.84E−3	28	$e(k-9)$	2.14E−1	2.18E−3
7	$x(k-8)$	1.47E−3	4.21E−3	18	$y^2(k-6)$	4.03E+0	2.71E−3	29	$e^4(k-2)$	−1.23E+3	2.12E−3
8	$x(k-2)$	1.70E−3	3.96E−3	19	$y^2(k-11)$	−1.14E+0	2.69E−3	30	$e^4(k-3)$	1.88E+4	2.11E−3
9	$x(k-9)$	−7.11E−4	3.75E−3	20	$y(k-5)$	−5.79E−2	2.59E−3	31	$e^2(k-2)$	2.43E−1	2.05E−3
10	$x(k-7)$	−6.59E−4	3.64E−3	21	$e^3(k-3)$	8.93E+2	2.55E−3	32	$e(k-2)$	1.77E−1	2.03E−3
11	$x(k-5)$	1.40E−4	3.56E−3	22	$e^3(k-10)$	1.19E+2	2.50E−3	33	$e^4(k-1)$	−1.88E+4	1.92E−3
								34	$e(k-5)$	9.57E−2	**1.91E−3**

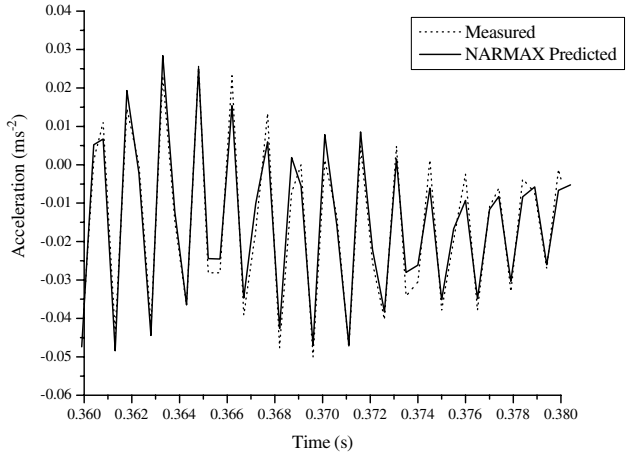

Fig. 8. The output of NARMAX model of the response to sinusoidal sweep excitation for the composite system.

well suited to model the input/output behavior of the multi-layer composite plate dynamics.

5. Delamination assessment using NARMAX model

5.1. Extraction of damage features

The NARMAX approach is a parametric estimation methodology for identifying both the structure and the parameters of an unknown nonlinear system. For a given composite system, the parameter class of the model is identical. If some physical property changes in the system, e.g., internal damage occurs in the composite plate, the model parameters estimated using measured input/output data are different from those of the intact system. Thus, the change of model parameter class can be a representation of the damage features in the composite system.

As the differences of signals between intact and damaged structures are generally insignificant in the early stage of damage, extraction of damage index directly from the parameter change is difficult. Therefore, the square of relative parameter change is used to enhance the sensitivity of features to damage. If θ_i^0 and θ_i^d represent coefficients of the NARMAX models associated with intact and damaged systems, respectively, the dimensionless index

$$\eta_i = \left(\frac{q_i^d - q_i^0}{q_i^0} \right)^2 \tag{15}$$

is adopted to demonstrate the feature of damage-induced parameter variation of the ith coefficient in the model. Therefore, according to the model of each damaged case, a series of columns can be plotted for η_i. Let the sum of all these columns be equal to 1 in a particular case, each of the columns can, therefore, represent the percentage of the total parameter variation for the considered damage case, i.e., the height of each column is

$$\zeta_i = \frac{\eta_i}{\sum_{i=1}^{n_\theta} \eta_i} \tag{16}$$

5.2. Experimental analysis on parameters of NARMAX model

5.2.1. Parameter change with damage severity

Four damaged composite plates have been fabricated, and named as Plates A, B, C and D, respectively. Each damaged plate has only one rectangular delamination located at the position with the center as shown in Fig. 1. The delamination areas of Plates A, B, C and D are 18×12, 36×24, 54×36 and 72×48 mm^2, respectively.

During experiment, the excitation signal and boundary conditions as well as the test set-up are the same for the intact and damaged plates. The input/output data are used to estimate the parameters of NARMAX model with the same structure and terms as those of the intact system. Fig. 9 shows the parameter variations for each delaminated plate. It is seen that when there is delamination in the plate, even as small as 0.5% of the whole plate area, the parameter change in the NARMAX model can still be observed. However, not all parameters have the same extent of change for different delamination areas, only some of them are especially significant. When the delamination is small, e.g., in Plates A and B, the number of the varied coefficients is very limited and the variation of different coefficients is nearly identical, but with the increase of delamination area more and more coefficients vary. Therefore, according to the variation manner of coefficients in the

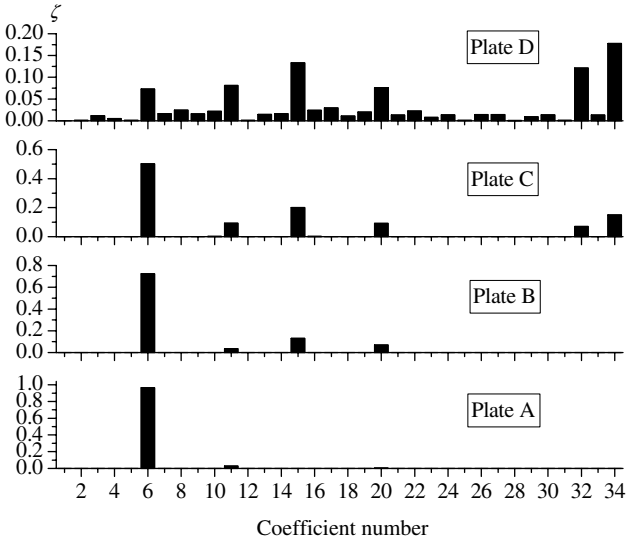

Fig. 9. Parameter variations in NARMAX model induced by delaminations of different areas in the composite plates.

NARMAX model of the composite system, the internal delamination can be fund and assessed.

5.2.2. Parameter change with damage location

In order to further investigate the distribution of varying parameters in NARMAX model five cantilever composite plates are also prepared, one is intact and four named E, F, G and H, respectively, are damaged. They are the same as those described in Section 5.2.1 except that their width is as shown in Fig. 10. Each damaged plate is delaminated at a specified region with an identical delaminated area. The damage locations of Plates E, F, G and H are also shown in Fig. 10.

After static and dynamic investigation on the nature of nonlinearity for the intact cantilever composite plate the term and coefficients of NARMAX model are estimated as shown in Table 4. The input signal excites the piezoelectric patch bonded on the top surface near the fixed end of the plate (the center of the bounded area is just at the point with coordinates $x = 18$ and $y = 45$), and the output data are measured by the accelerometer adhered to the point as shown in Fig. 10.

Using Eqs. (15) and (16) for each damaged cantilever plate, the delamination-induced change of parameters in NARMAX model can be computed, and the input/output data are used to estimate coefficients of the model with the same structure and terms as that for the intact plate. Fig. 11 shows parameter variations for each delaminated plate. It is seen that quite a lot of coefficients vary for each damaged plate when the delaminated region is as large as 9% of the whole plate area. It is also obvious that the variation distribution of coefficients is different when delamination locates at different regions. The maximum variation occurs in different coefficients for plates with different damage locations. Therefore, it is practical to identify damage location according to the variation distribution of coefficients in NARMAX model, but further investigation is necessary for much more samples.

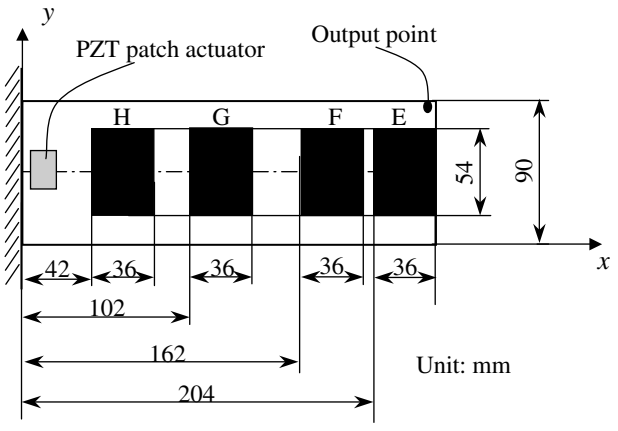

Fig. 10. Delamination locations and dimensions of the cantilever plates.

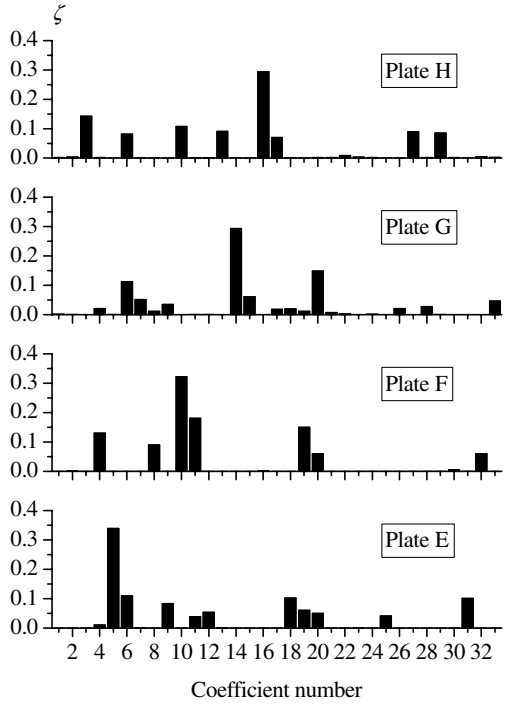

Fig. 11. Parameter variations in NARMAX model induced by delaminations at different locations in the cantilever plates.

Table 4
Results of NARMAX model estimation for the intact cantilever plate

i	$p_i(k)$	θ_i	err	i	$p_i(k)$	θ_i	err	i	$p_i(k)$	θ_i	err
1	$y(k-9)$	−8.88E−2	1.02E+0	12	$x(k-3)$	1.88E−2	2.45E−1	23	$e(k-5)$	4.41E−1	1.62E−1
2	$y(k-4)$	−1.40E+0	8.37E−1	13	$y(k-8)$	1.02E−1	2.16E−1	24	$e(k-3)$	3.56E−1	1.58E−1
3	$y(k-2)$	−1.13E+0	6.83E−1	14	$y^4(k-3)$	4.96E−2	2.17E−1	25	$e(k-6)$	2.90E−1	1.53E−1
4	$x(k-2)$	−1.66E−2	6.48E−1	15	$y^4(k-4)$	7.74E−3	2.18E−1	26	$e^2(k-6)$	4.58E−1	1.50E−1
5	$x(k-7)$	5.00E−4	6.12E−1	16	$y(k-5)$	1.06E+0	2.12E−1	27	$e^3(k-5)$	−8.18E+1	1.47E−1
6	$x(k-1)$	4.70E−3	5.76E−1	17	$e^3(k-1)$	−5.33E+0	1.98E−1	28	$e^2(k-1)$	−3.71E+0	1.47E−1
7	$y(k-7)$	−1.26E−1	5.47E−1	18	$e^4(k-4)$	−1.39E+0	1.88E−1	29	$e(k-2)$	−1.62E−1	1.45E−1
8	$y(k-3)$	9.57E−1	4.46E−1	19	$e^2(k-3)$	1.25E+0	1.79E−1	30	$e^3(k-8)$	3.21E−1	1.43E−1
9	$x(k-4)$	−7.35E−3	4.04E−1	20	$e^4(k-2)$	−9.80E−1	1.74E−1	31	$e(k-1)$	−1.15E−1	1.41E−1
10	$y(k-1)$	1.57E+0	3.65E−1	21	$e(k-8)$	−3.35E−1	1.69E−1	32	$e(k-9)$	−3.04E−1	1.39E−1
11	$y(k-6)$	−6.63E−2	2.65E−1	22	$e^4(k-5)$	−8.94E+1	1.67E−1	33	$e^3(k-9)$	4.08E−1	1.36E−1

6. Conclusions

A complete but elementary damage detection methodology for a composite vibration system is presented in this paper. Both static and dynamic investigations on nonlinear nature of the system are carried out. Then, the structure of the nonlinear discrete model is identified using the measured input/output data by analysis on mean square errors of forward order and time delay in linear model. Parameters in the NARMAX model of the undamaged composite system is then estimated and validated. Finally, the structure of the proposed model is used to estimate model parameters for damaged vibration systems, and internal delamination is detected by comparing model parameters between intact and damaged systems. Results show that it is effective and practical to investigate dynamic behavior and to assess damage in composite system by means of analysis on properties of NARMAX model. This paper contributes to not only the understanding of the use of parametric identification method for modeling of composite vibration systems, but also the exploration of internal damage detection, especially in the early stage, for composite systems.

Acknowledgements

The work described in this paper is supported by the Research Grants Council of Hong Kong Special Administrative Region, China (Project no. PolyU 5174/01E and PolyU 5313/03E). The authors are also grateful for the support of The Hong Kong Polytechnic University to carrying out this project.

References

[1] Tasi SW, Hann HT. Introduction to composite materials. Westport, Connecticut: Technic Publishing Company; 1980.
[2] Gerardi TG. Health monitory aircraft. J Intell Mater Syst Struct 1990;1:375–85.
[3] Voyiadjis GZ. Damage in composite materials. Amsterdam, New York: Elsevier; 1993.
[4] Gadelrab RM. The effect of delamination on the natural frequencies of a laminated composite beam. J Sound Vibrat 1996;197(3):283–92.
[5] Osset Y, Roudolff F. Numerical analysis of delamination in multilayered composite plates. Comput Mech 2000;20(1–2):122–6.
[6] Zou Y, Tong L, Steven GP. Vibration-based model-dependent damage (delamination) identification and health monitoring for composites structures. J Sound Vibrat 2000;230:357–78.
[7] Caelli TM, Squire DM, Wild TPJ. Model-based neural networks. Neural Networks 1993;6(5):613–25.
[8] Lin SH, Kung SY, Lin LJ. Face recognition/detection by probabilistic decision-based neural networks. IEEE Trans Neural Networks 1997;8(1):114–32.
[9] Perlovsky LI et al. Model-based neural network for target detection in SAR images. IEEE Trans Image Process 1997;6(1):203–16.
[10] Leontaritis IJ, Billings SA. Input–output parametric models for nonlinear systems. Int J Control 1985;41(2):303–44.
[11] Billings SA, Tsang KM. Spectral analysis of nonlinear systems—Part I. Parametric nonlinear spectral analysis. J Mech Syst Signal Process 1989;3(4):319–39.
[12] Evans C, Rees D, Hill D. Frequency-domain identification of gas turbine dynamics. IEEE Trans Control Syst Technol 1998;6(5):651–62.
[13] Korenberg MJ, Billings SA, Liu YP. An orthogonal parameter estimation algorithm for nonlinear stochastic systems. Int J Control 1988;48:193–210.
[14] Billings SA, Korenberg MJ, Chen S. Identification of nonlinear output-affine systems using an orthogonal least squares algorithm. Int J Syst Sci 1988;19:1339–568.